Entropy cascade and temporal intermittency in a shell model for convective turbulence

Eri Suzuki and Sadayoshi Toh
Department of Physics, Faculty of Science, Kyoto University, Kyoto 606-01, Japan
(Received 22 June 1994; revised manuscript received 1 March 1995)

The statistical nature of convective turbulence is numerically studied in a shell model under the assumption of neutrally stable stratification. The entropy (T^2) cascade and the inverse transfer of the kinetic energy are confirmed with flux and transfer functions. It is also shown that the entropy and the energy spectra for different values of diffusivity agree well with universal functions involving the power-law ranges derived by Bolgiano and Obukhov. The anomalous scaling of the exponents of "structure functions" suggests the existence of temporal intermittency in convective turbulence, which is similar to that in three-dimensional isotropic Navier-Stokes turbulence. The intermittency, however, is not explained well by multifractal cascade models modified for convective turbulence.

PACS number(s): 47.27.Eq, 47.27.Gs, 47.27.Te

I. INTRODUCTION

Hard turbulence is fully developed convective turbulence found by Libchaber and co-workers [1–4]. It has several features that differ from those of traditional convective turbulence (soft turbulence). Among these features, the following is noteworthy: large-scale cell flow starts just after fully developed turbulence sets in. According to experiments in the hard turbulence regime, a frequency power spectrum of temperature fluctuations recorded at the center of an experimental box contains a power law range with an exponent close to $-7/5$ [3,4] (what is called the entropy spectrum [5]). This power law was derived by Bolgiano and Obukhov for thermal turbulence in stably stratified fluid in 1959 (BO scaling) [6]. L'vov, Procaccia and Zeitak, and Yakhot found the same scaling theoretically [5,7,8]. In particular, L'vov obtained BO scaling by assuming that entropy T^2, which is one of the conserved quantities in the inviscid limit, is cascaded to smaller scales. In this way, in the central region of the experimental box the convective turbulence is assumed to be fully developed and isotropic.

How is the robust circulation flow surrounding the central region maintained? From the results so far, we have inferred that one of the maintenance mechanisms is the energy supply from the central region. In this region the entropy supplied from the surrounding region is converted into kinetic energy through the entropy cascade. This energy supply cannot be enough to maintain the flow; however, it may at least play a role in rectifying the flow.

Brandenburg studied the relation between BO scaling and the direction of the energy transfer, introducing a shell model on the basis of the Boussinesq approximation [9]. In his model, nonlinear terms in the evolution equation of velocity are roughly divided into two groups. One group causes the kinetic energy to transfer to smaller scales and the other to larger scales. He showed that if the latter group exceeds the former, BO scaling can appear, that is, BO scaling is closely connected to the inverse transfer of kinetic energy. This conclusion is also supported by our two-dimensional (2D) free convection model based on the Boussinesq approximation equation [10].

Little research has been carried out on intermittency in convective turbulence. The only work we are aware of has been on multifractal scaling of the entropy spectrum [4]. Wu *et al.* found that the frequency spectra of entropy for different values of the Rayleigh number Ra coincide well not by simple BO scaling but by multifractal scaling. The multifractal model predicts not only the anomalous behavior of the scaling exponents for higher order structure functions, but also the existence of the intermediate dissipation range in the energy spectrum [12]. Multifractal scaling is required to describe this intermediate dissipation range.

In this paper, we will study how entropy and kinetic energy are transferred in the wave-number space, focusing in particular on the intermittent nature of the transfer processes.

In Sec. II, we will review the 2D free convection model on which our shell model is based. Bolgiano-Obkhov scaling is also reviewed there. In Sec. III, we will modify the shell model proposed by Brandenburg in order to bring it close to our 2D model of the central region. On the other hand, Brandenburg tried to model the whole system, including the central region and surroundings. Moreover, the temperature field is forced at all scales by the background linear stratification. Thus, interpretation of the spectra requires some care. However, the basic results are not affected crucially and our work is based strongly on Brandenburg's results. Through our modified model, the universality of BO scaling is shown. The direction of energy and entropy is also examined in terms of transfer and flux functions.

In Sec. IV, the intermittent nature of temperature and velocity dynamics are examined by structure functions and compared with multifractal cascade models such as the random-β model [14]. In the final section, we conclude with some remarks.

II. PRELIMINARY

A. Free convection model

To examine the characteristics of fully developed convective turbulence, we proposed a model situation where the central region is separated from surrounding flows such as boundary and mixing layers [10]. The effect of the surroundings on the central region is taken into account only through the forcing of temperature dynamics. In fact, entropy seems to be supplied to the central region by random intrusion of plumes. We also assumed neutrally stable stratification and homogeneity. These assumptions are supported by the 3D experiments and our 2D simulations [11]. The model is based on the following 2D Boussinesq approximation equations with several terms representing the assumptions:

$$\frac{\partial T}{\partial t} = -\boldsymbol{u}\cdot\boldsymbol{\nabla}T + \kappa\nabla^2 T + F, \tag{1}$$

$$\frac{\partial \boldsymbol{u}}{\partial t} = -\boldsymbol{u}\cdot\boldsymbol{\nabla}\boldsymbol{u} - \boldsymbol{\nabla}p + \nu\nabla^2\boldsymbol{u} + \alpha\boldsymbol{g}T + \boldsymbol{D}, \tag{2}$$

$$\boldsymbol{\nabla}\cdot\boldsymbol{u} = 0, \tag{3}$$

where κ, ν, α, and $\boldsymbol{g}$ are the thermal diffusivity, the kinematic viscosity, the volume expansion coefficient, and the gravitational acceleration, respectively, and F and $\boldsymbol{D}$ denote forcing and drag. Only the temperature field is forced at large scales. The energy sink, $\boldsymbol{D}$ is also added only for large scales to keep the system statistically stationary.

In the inviscid limit, this system conserves the entropy $\mathcal{S} = \int \frac{1}{2}T^2 dV$ and the total energy $\mathcal{E}_t = \int(\frac{1}{2}|\boldsymbol{u}|^2 + \alpha g y T)dV$, where the buoyancy acts along the y direction. Numerical simulations showed the existence of Bolgiano-Obkhov scaling due to the entropy cascade and the inverse transfer of kinetic energy. It was also shown that both entropy and kinetic energy are distributed isotropically at small scales, including inertial range, even though the system has buoyancy. This supports Kolmogorov-type scaling.

B. Bolgiano-Obkhov scaling

Here we will summarize BO scaling. As a generalization of the Kolmogorov hypothesis to the case of neutrally stratified thermal turbulence, we assume that statistical natures are governed by the parameters ϵ_θ, αg, κ, and ν, where ϵ_θ is the entropy dissipation rate. Using this hypothesis and applying simple dimensional analysis, the entropy and energy spectra are written in the following forms:

$$S(k) = \kappa^{7/8}(\alpha g)^{-3/4}\epsilon_\theta^{5/8}\mathcal{F}(k/k_{\theta_d}), \tag{4a}$$

$$E(k) = \nu^{11/8}(\alpha g)^{1/4}\epsilon_\theta^{1/8}\mathcal{G}(k/k_d). \tag{4b}$$

Here, $\mathcal{F}(k/k_{\theta_d})$ and $\mathcal{G}(k/k_d)$ are expected to be universal functions, although they may depend on the Prandtl number $\mathrm{Pr}=\nu/\kappa$. Dissipation cutoff wave numbers k_{θ_d} and k_d are given by

$$k_{\theta_d} = \kappa^{-5/8}(\alpha g)^{1/4}\epsilon_\theta^{1/8}, \tag{5a}$$

$$k_d = \nu^{-5/8}(\alpha g)^{1/4}\epsilon_\theta^{1/8}. \tag{5b}$$

In the inertial range, the spectra depend only on ϵ_θ, αg, and k; then

$$S(k) = C_S(\alpha g)^{-2/5}\epsilon_\theta^{4/5}k^{-7/5}, \tag{6a}$$

$$E(k) = C_E(\alpha g)^{4/5}\epsilon_\theta^{2/5}k^{-11/5}, \tag{6b}$$

where C_S and C_E are also expected to be universal constants. It should be noted that this phenomenological theory does not give the direction of the energy transfer in the wave-number space.

III. MODEL EQUATIONS AND BASIC RESULTS

In this section we present an improved shell model for convective turbulence and basic numerical results. The model is constructed in a discretized wave-number space where the nth wave number is defined by $k_n = k_0 h^n (1 \le n \le N)$, and k_0 is the wave number corresponding to the largest possible scale in the system. In this paper, we use the customary values $k_0 = 1$ and $h = 2$. Scalar variables u_n and T_n represent $\boldsymbol{u}$ and T on the nth shell in the wave-number space. The entropy and kinetic energy spectra are therefore defined as $S(k_n) = T_n^2/(2k_n)$ and $E(k_n) = u_n^2/(2k_n)$. Each evolution equation for u_n or T_n is assumed to be coupled quadratically with the nearest neighbors in the wave-number space. Then the evolution equations for u_n and T_n are

$$\frac{dT_n}{dt} = F_T(k_n) - \kappa k_n^2 T_n + f\delta_{n,4}, \tag{7}$$

$$\frac{du_n}{dt} = F_u(k_n) - \nu k_n^2 u_n + \alpha g T_n - \frac{1}{k_n^2}\tilde{f}\delta_{n,i}u_n \quad (i = 1,2,3,4), \tag{8}$$

where

$$F_T(k_n) = k_n \sum_{i,j=0,\pm1} a_{ij} u_{n+i} T_{n+j}, \tag{9a}$$

$$F_u(k_n) = k_n \sum_{i,j=0,\pm1} b_{ij} u_{n+i} u_{n+j}. \tag{9b}$$

Here, $f\delta_{n,4}$ is the forcing term and $-\tilde{f}\delta_{n,i}u_i/k_n^2$ is the drag term. We used $f = 10^3$ and $\tilde{f} = 0.5$. Both the forcing and the drag are adopted for keeping the system statistically stationary. We can put $\alpha g = 1$ without loss of generality. The coupling coefficients a_{ij} and b_{ij} are determined by the conditions where the entropy and the total energy are conserved in the inviscid limit without forcing and drag:

$$\frac{d}{dt}\sum_{n=1}^{N}\frac{1}{2}T_n^2 = 0, \tag{10}$$

$$\frac{d}{dt}\sum_{n=1}^{N}\frac{1}{2}u_n^2 - \alpha g\sum_{n=1}^{N}T_n u_n = 0. \tag{11}$$

Then we obtain the following forms:

$$F_T(k_n) = A_1 k_n(u_{n-1}T_{n-1} - hu_nT_{n+1}) + A_2 k_n(u_nT_{n-1} - hu_{n+1}T_{n+1}), \tag{12a}$$

$$F_u(k_n) = B_1 k_n(u_{n-1}^2 - hu_nu_{n+1}) + B_2 k_n(u_nu_{n-1} - hu_{n+1}^2), \tag{12b}$$

where A_1, A_2, B_1, and B_2 are arbitrary constants. Brandenburg indicated that the ratios $|A_2/A_1|$ and $|B_2/B_1|$ are related to the relative importance of entropy and kinetic energy transfer. He reported that Kolmogorov scaling was seen when the ratio $|B_2/B_1|$ is some critical value (around 0.4). We therefore used $B_1 = 0.01$, $A_1 = A_2 = B_2 = 1$; this choice is the same as he used.

We deal with the interactions only with the nearest neighbors. However, even if the interactions with the next-nearest neighbors are also included, the numerical results are not greatly affected.

In our calculation, we treat the case $\kappa = \nu(Pr = 1)$. We mostly used the values of the parameters $\kappa = \nu = 10^{-14}$, $N = 40$. Time marching was performed by the fourth-order Runge-Kutta method with time step $dt = 2\times10^{-7}$. Statistical quantities are obtained by averaging over 1.3×10^9 steps.

Figure 1 shows the entropy and energy spectra $S(k)$ and $E(k)$. We see that the power-law behavior of the spectra agree well with BO scaling: $S(k) \propto k^{-7/5}$ and $E(k) \propto k^{-11/5}$. To confirm the agreement with BO scaling, we plot $k^{7/5}S(k)$ and $k^{11/5}E(k)$ in an inset of Fig. 1. In the wave-number range $10^2 < k < 10^7$ these values are not strictly constant but decrease slightly as the wave numbers increase. This is because the actual powers of $S(k)$ and $E(k)$ are -1.42 and -2.23. Both of the differences between these values and the powers predicted by BO scaling are only 1.4% and the spectra satisfy BO scaling very well. In addition, both of the spectra have steeper slopes, -1.69 and -2.42, than those predicted by BO scaling in the wave-number range $10^7 < k < 10^9$. The straight lines in the inset correspond to these powers. When we used hyperviscosity, this range disappeared and only the BO power law was observed. Here we only imply that this extra range is related to the dissipation. The details will be reported elsewhere.

Figure 2 shows the normalized spectra $\mathcal{F}(k/k_{\theta_d})$ and $\mathcal{G}(k/k_d)$ for different values of κ and ν. The entropy and energy spectra for different parameter values coincide well with BO scaling. Therefore, this figure supports BO scaling and the existence of universal functions, although the universal functions should depend on the Prandtl number Pr. As mentioned in Sec. I, Wu *et al.* reported that the frequency spectra coincide well over the whole range by multifractal scaling, by not by BO scaling, for extremely large Rayleigh numbers [4], although this does not hold for our model. As a matter of fact, we tried to compare the spectra with multifractal scaling, but failed. Though only the inertial range is, of course, fitted well by both BO scaling and multifractal scaling, the spectra that included the dissipation range were not fitted well with the latter. So far we cannot clearly account for the failure of multifractal scaling in our model. Here we only suggest that shell models may not reproduce the dissipation range clearly. For example, the shell model for the 3D Navier-Stokes turbulence by Yamada and Ohkitani does not show exponential decay such as $E(k) \sim \exp(-ck)$, although our model contains the exponentially decaying range.

The entropy and energy flux functions are defined as $\Pi_S(k_n) = -\sum_{i=1}^{n}F_T(k_i)T_i$ and $\Pi_E(k_n) = -\sum_{i=1}^{n}F_u(k_i)u_i$. From a dimensional consideration, the flux function of the kinetic energy obeys the following

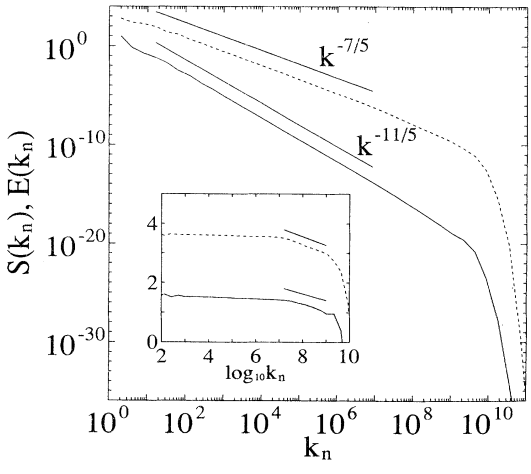

FIG. 1. Entropy (dashed line) and energy spectra (solid line) for $\kappa = \nu = 10^{-14}$ with $N = 40$. The straight lines show the slopes predicted by BO scaling. The inset shows $k_n^{7/5}S(k_n)$ (dashed line) and $k_n^{11/5}E(k_n)$ (solid line). The straight lines correspond to the powers -1.69 and -2.42.

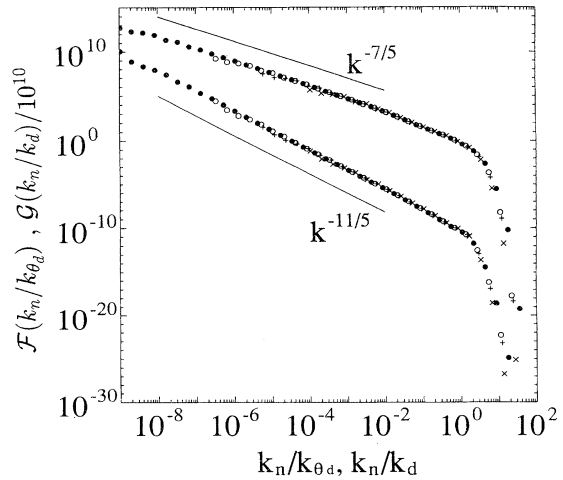

FIG. 2. The normalized spectra $\mathcal{F}(k_n/k_{\theta_d})$ (upper) and $\mathcal{G}(k_n/k_d)$ (lower) for $\kappa = \nu = 10^{-14}(\bullet)$, $10^{-10}(\circ)$, $10^{-8}(+)$, $10^{-6}(\times)$. The energy spectra are divided by 10^{10}. The solid lines show the slopes predicted by BO scaling.

power law in the inertial range [5]:

$$\Pi_E(k) \propto k^{-4/5}. \tag{13}$$

Figure 3 is the plot of $\log_{10}|\Pi_E(k)|$ vs $\log_{10} k$. The flux function of the kinetic energy agrees with the power-law predicted by (13).

In our 2D simulations we observed the entropy cascade and the inverse transfer of kinetic energy. In this shell model the same phenomena are seen. As shown in Fig. 4, the energy flux is negative and the entropy flux is positive and constant over the wave-number range where the spectra obey BO scaling. These results indicate the presence of both the entropy cascade and the inverse transfer of kinetic energy in the inertial range. It should be noted that kinetic energy is not cascaded but transferred to larger scales.

Buoyancy plays an important role in the energy transfer process. We will explain this role using the evolution equation for kinetic energy:

$$\frac{dE(k_n)}{dt} = \mathcal{T}_E(k_n) + \mathcal{L}(k_n) + \mathcal{D}(k_n) - \frac{1}{k_n^2}\tilde{f}\delta_{n,i}E(k_n) \quad (i = 1, 2, 3, 4). \tag{14}$$

Here, $\mathcal{T}_E(k_n)$, $\mathcal{L}(k_n)$, and $\mathcal{D}(k_n)$ are the kinetic energy transfer function, the linear term due to the buoyancy effect, and the dissipation term, respectively. They are defined as $\mathcal{T}_E(k_n) = F_u(k_n)u_n$, $\mathcal{L}(k_n) = \alpha g T_n u_n$, and $\mathcal{D}(k_n) = -\nu k_n^2 u_n^2$. Dissipation is negligible in the inertial range, so that the transfer function and the linear term are balanced on average; $\langle \mathcal{T}_E(k_n)\rangle = \langle -\mathcal{L}(k_n)\rangle$ (see Fig. 5). In addition, in the inertial range the value of the transfer function is negative, and that of the linear term is positive. These indicate that potential energy is converted to kinetic energy on average through buoyancy.

IV. INTERMITTENT NATURE OF STRUCTURE FUNCTIONS

In this section, we will examine the intermittent nature of the convective turbulence in terms of structure functions. We also try to extend multifractal cascade models to the convective turbulence.

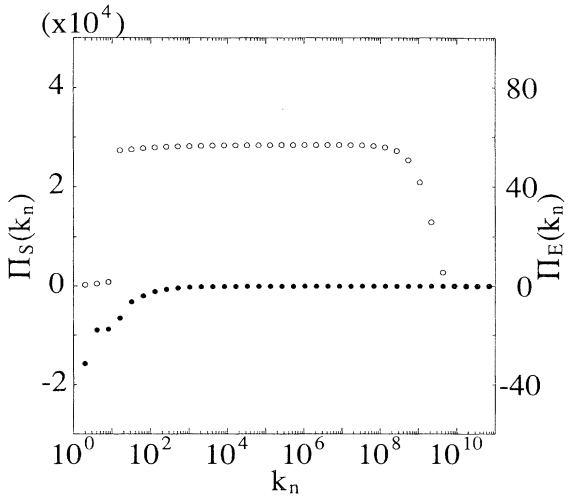

FIG. 4. Entropy and energy flux functions $\Pi_S(k_n)$ (○) and $\Pi_E(k_n)$ (●) for $\kappa = \nu = 10^{-14}$.

The scaling exponents of the structure functions, $\zeta_T(p)$ and $\zeta_u(p)$ are defined as follows:

$$\langle \delta T(r)^p \rangle \propto r^{\zeta_T(p)}, \tag{15a}$$

$$\langle \delta u(r)^p \rangle \propto r^{\zeta_u(p)}, \tag{15b}$$

where $\delta T(r) = |T(x+r) - T(x)|$, $\delta u(r) = |u(x+r) - u(x)|$, r is the spatial difference of the length in the inertial range, and $\langle\,\rangle$ indicates time average. From BO scaling, δT and δu are assumed to be determined by αg, ϵ_θ, and r, so that the structure functions have the following forms:

$$\langle \delta T(r)^p \rangle \propto (\alpha g)^{-p/5} \epsilon_\theta^{2p/5} r^{p/5}, \zeta_T(p) = p/5, \tag{16a}$$

$$\langle \delta u(r)^p \rangle \propto (\alpha g)^{2p/5} \epsilon_\theta^{p/5} r^{3p/5}, \zeta_u(p) = 3p/5. \tag{16b}$$

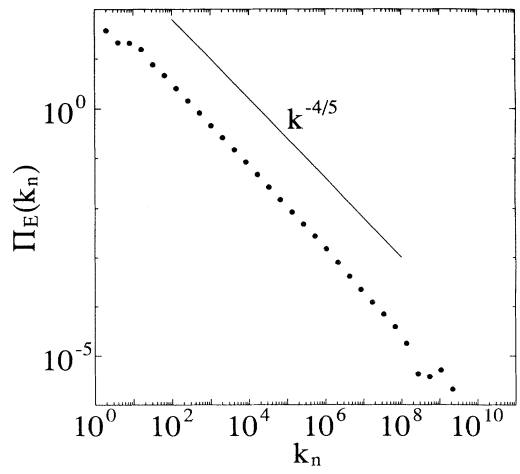

FIG. 3. A plot of $\log|\Pi_E(k_n)|$ vs $\log k$ for $\kappa = \nu = 10^{-14}$. The solid line shows the slope $-4/5$.

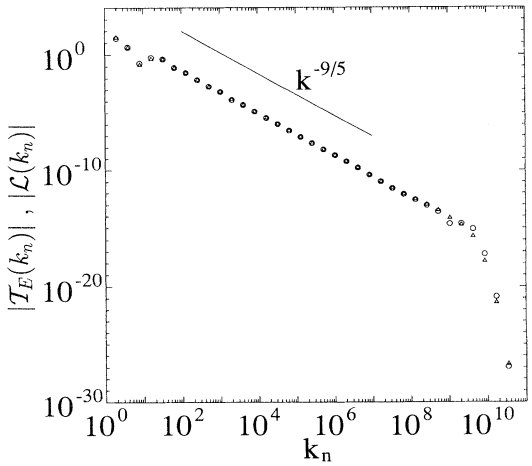

FIG. 5. The kinetic energy transfer function $|\mathcal{T}_E(k_n)|$ (○) and the linear term $|\mathcal{L}(k_n)|$ (△) for $\kappa = \nu = 10^{-14}$. In the inertial range, $\langle \mathcal{L}(k_n)\rangle \simeq -\langle \mathcal{T}_E(k_n)\rangle > 0$.

We have calculated the temperature and velocity structure functions, $\langle|T_n|^p\rangle$ and $\langle|u_n|^p\rangle$, for positive integers up to $p = 12$. Figure 6 shows the plots of $\langle|T_n|^p\rangle$ and $\langle|u_n|^p\rangle$ with k_n for $p = 10$. Both of the structure functions have less steep slopes than those predicted by BO scaling. As shown in Fig. 7, the scaling exponents of the structure functions $\zeta_T(p)$ and $\zeta_u(p)$ are smaller than those expected from BO scaling. The behavior of the scaling exponents similar to ours is reported in three-dimensional isotropic turbulence; the scaling exponents, because of intermittency, are smaller than those expected from Kolmogorov scaling.

The convergence of the exponents of the structure functions should be confirmed carefully especially for higher orders. We calculated the probability distribution functions (PDFs) of temperature differences T_n at several scales to estimate the convergence of the structure functions. Figures 8 and 9 show the PDF $P(T_n)$ and the function $W_p(T_n) \equiv T_n^p P(T_n)$ for $p = 10$ and $n = 17$ at the middle of the inertial range. As shown in Fig. 9, even for $p = 10$ we can see clear peaks and decaying tails in $W_p(T_n)$. A similar tendency was seen at other scales $n = 10, 14, 20, 24$. For $p > 10$ the peaks are almost at the cutoff values of $W_p(T_n)$ and sufficiently decaying tails are not seen. The PDFs are fitted well by stretched-exponential forms $P(T_n) = P(0)\exp(-c|T_n|^\beta)$ (see Fig. 8). In terms of these approximated PDFs, we also estimated the structure functions and their exponents. The results are also shown in Figs. 6 and 7. We see that both of them show values not very different from the values obtained from direct calculation. In addition, we have calculated the exponents for averages over another 1.2×10^8 steps, although the results are no different from those shown in Fig. 7. Based on these considerations, we believe that the exponents of the structure functions converge enough at least for $p \leq 10$.

The scaling exponents for the velocity structure functions calculated with a shell model for isotropic turbulence are well fitted with the random-β model [13]. We also try to fit the exponents by the random-β model. Multifractal cascade models such as the random-β model assume the kinetic energy cascade. Thus we assume the entropy cascade in order to apply these cascade models to our shell model. That is, we assume that the rate of entropy transfer is constant between the length scales r_n and r_{n+1},

$$u_n T_n^2 / r_n \simeq \beta_{n+1} u_{n+1} T_{n+1}^2 / r_{n+1}, \tag{17}$$

where $r_n = 2^{-n} r_0$, and β_n is the rate of active regions. In

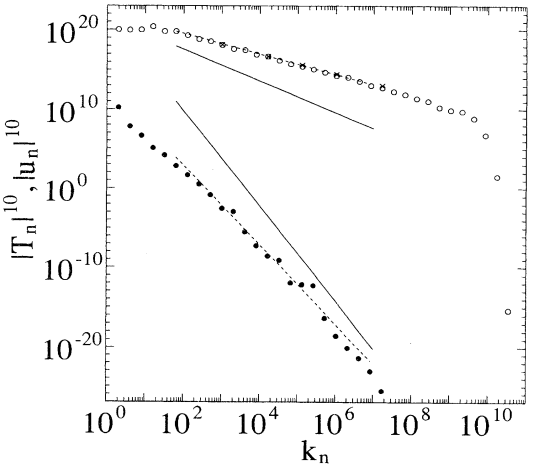

FIG. 6. Entropy and kinetic energy structure functions $|T_n|^{10}$ (○) and $|u_n|^{10}$ (●) for $\kappa = \nu = 10^{-14}$. The solid lines indicate the BO scaling law. The broken lines with slopes 5.10 (lower) and 1.28 (upper) are least-squares fits. The structure functions estimated from the stretched exponential fitting of PDF (×).

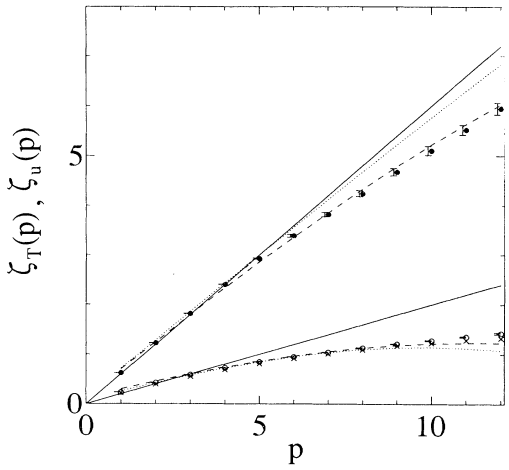

FIG. 7. The scaling exponents of the structure functions $\zeta_T(p)$(○) and $\zeta_u(p)$(●). The solid lines are the BO prediction $\zeta_T(p) = p/5$ and $\zeta_u(p) = 3p/5$. The error bars of the scaling exponents are estimated from least-squares fits of the structure functions. The scaling exponents estimated from the stretched exponential fitting of PDF (×). The dotted lines are least-squares fits up to $p = 12$ in terms of (22a) and (22b) with $x = 0.116$. The broken lines are least-squares fits up to $p = 12$ in terms of (24a) and (24b) with $x = 0.178$. This result is obtained for $\kappa = \nu = 10^{-14}$.

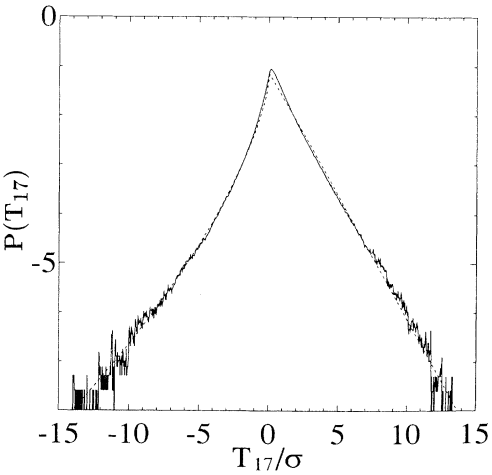

FIG. 8. PDF (solid line) and stretched exponential fitting (broken line) of $P(T_{17})$ for $\kappa = \nu = 10^{-14}$. PDF is normalized by the standard deviation $\sigma = \langle|T_{17}|^2\rangle^{1/2}$.

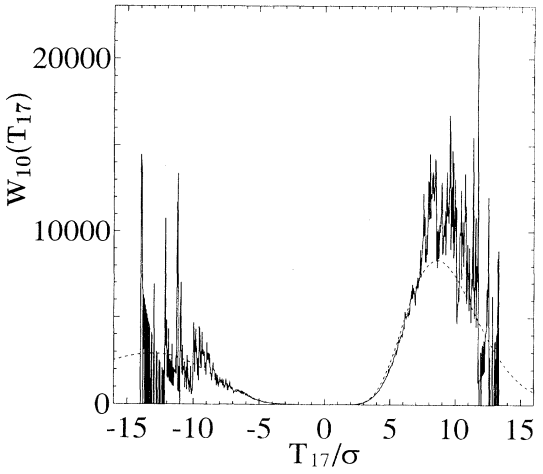

FIG. 9. $W_{10}(T_{17})$ for $\kappa = \nu = 10^{-14}$ (solid line). The broken line is $W_{10}(T_{17})$ corresponding with the stretched exponential form in Fig. 8. The same scale as in Fig. 8 is used for the abscissa.

the active region, the transfer process mainly occurs. In addition, we assume local balance of the nonlinear term with the buoyancy term in (8),

$$\alpha g T_n \simeq u_n^2 / r_n. \tag{18}$$

This assumption is supported by our shell model and 2D simulations (see Fig. 5). From these assumptions, T_n and u_n are estimated as follows:

$$T_n \sim \left(\prod_{i=1,n} \beta_i \right)^{-2/5} r_n^{1/5}, \tag{19a}$$

$$u_n \sim \left(\prod_{i=1,n} \beta_i \right)^{-1/5} r_n^{3/5}. \tag{19b}$$

For simplicity, assuming that there are no correlations among different steps of the fragmentation process, we obtain

$$\langle |T_n|^p \rangle = r_n^{p/5} \left\langle \beta^{1-2p/5} \right\rangle, \tag{20a}$$

$$\langle |u_n|^p \rangle = r_n^{3p/5} \left\langle \beta^{1-p/5} \right\rangle. \tag{20b}$$

If we use the probability distribution $P(\beta)$ written in the form

$$P(\beta) = x\delta(\beta - a) + (1 - x)\delta(\beta - b), \tag{21}$$

the exponents of the structure functions are given as follows:

$$\zeta_T(p) = \frac{1}{5}p - \log_2(xa^{1-2p/5} + (1-x)b^{1-2p/5}), \tag{22a}$$

$$\zeta_u(p) = \frac{3}{5}p - \log_2(xa^{1-p/5} + (1-x)b^{1-p/5}), \tag{22b}$$

where a and b are fragmentation parameters with probability x and $1-x$, respectively. In the original random-β model, $a = 0.5$ (velocity sheets), $b = 1$ (space-filling disturbance), and x is the only free parameter [14].

Figure 10 shows the deviations in scaling exponents from the values of BO scaling, $\Delta\zeta_T(p) = \frac{1}{5}p - \zeta_T(p)$ and $\Delta\zeta_u(p) = \frac{3}{5}p - \zeta_u(p)$. The broken lines are least-squares fits up to $p = 12$ in terms of (22a) and (22b) with $x = 0.116$. Other parameters are fixed at $a = 0.5$ and $b = 1$ following the original random-β model. This fitting does not work well. Even though we use a, b, and x as free parameters, we cannot fit both scaling exponents. Only $\zeta_T(p)$ or $\zeta_u(p)$ is fitted with this modified random-β model. The value of parameter b, however, is larger than unity, that is, $x = 0.780$, $a = 0.788$, and $b = 1.723$, when $\zeta_T(p)$ is fitted. The fits up to $p = 10$, where the scaling exponents converge enough, show similar tendencies.

We consider another modification of the random-β model. Here, instead of the relation (18), we assume the following one:

$$\alpha g T_n \simeq \eta_n u_n, \tag{23}$$

where η_n is a function of $k_n = 1/r_n$. This relation is based on the fact that both deviations of the exponents from those predicted by BO scaling are roughly the same (see Fig. 10). In the first model, the nonlinear term is as-

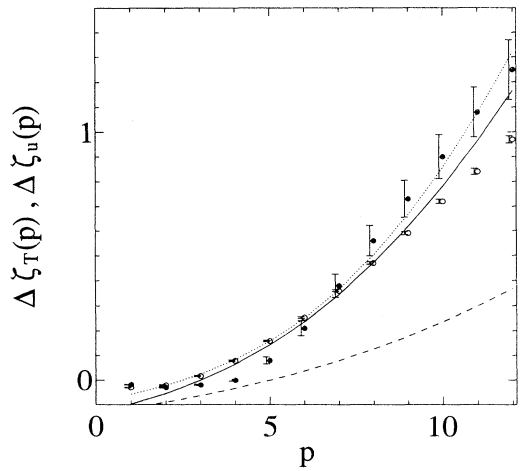

FIG. 10. The deviations in the exponents of the structure functions from the BO values, $\Delta\zeta_T(p)(\circ)$ and $\Delta\zeta_u(p)(\bullet)$. The error bars of the scaling exponents are estimated from least-squares fits of the structure functions. The dotted and broken lines are least-squares fits up to $p = 12$ in terms of (22a) and (22b) with $x = 0.116$. The solid line is least-squares fits up to $p = 12$ in terms of (24a) and (24b) with $x = 0.178$. This result is obtained for $\kappa = \nu = 10^{-14}$.

sumed to balance with the buoyancy term, which acts as the energy source on average. On the other hand, in this model, only part of the nonlinear term is assumed to balance with the buoyancy term. This may be understood easily if we introduce the "eddy viscosity": $\eta_n = -\nu_n k_n^2$, that is, the local energy input due to the buoyancy dominates energy transfer due to the nonlinear term. This situation is possible only when the energy is transferred to larger scales. Otherwise, the mean flux exceeds the energy supply, since the latter decreases with scale and the former is the sum of the latter over the scales from r_0 to r_n, the scale considered. It should be noted that the eddy viscosity is positive. Kraichnan derived the expression for the negative eddy viscosity within a closure framework for the energy inverse cascade of two-dimensional turbulence [15]. In his theory, the eddy viscosity is due to the nonlocal interactions, effects of much smaller scale. However, our eddy viscosity is not explicitly related to the energy inverse transfer, but only introduced to balance the local energy supply due to the buoyancy term; shell models deal with only local interactions. Thus our eddy viscosity is special but yields fascinating results. It should be noted that our eddy viscosity, too, is derived from nonlocal interactions as mentioned above.

From dimensional considerations, the coefficient of the eddy viscosity, ν_n, should vary as $r_n^{8/5+\delta}$, where δ represents the small deviation from the BO scaling. Adopting the procedure in the derivation of (22a) and (22b) with the assumptions (17) and (22w), we obtain another expressions for the exponents of the structure functions:

$$\zeta_T(p) = \left(\frac{1}{5} + \frac{1}{3}\delta\right)p - \log_2[xa^{1-p/3} + (1-x)b^{1-p/3}], \tag{24a}$$

$$\zeta_u(p) = \left(\frac{3}{5} - \frac{2}{3}\delta\right)p - \log_2[xa^{1-p/3} + (1-x)b^{1-p/3}]. \tag{24b}$$

We set $\delta = 0$ and fit both of the scaling exponents. The solid line in Fig. 10 is the least-squares fits with $x = 0.178$ ($a = 0.5$ and $b = 1$) by (24a) and (24b). This second model appears to work fairly well in comparison to the first one. This means that the eddy viscosity is an excellent model as the first approximation, though it is only introduced heuristically.

This model is not sufficient to fit both the scaling exponents in detail. In particular, it fails to explain the behavior of the low order moments. If $\delta = 0$, this model predicts that both deviations of the exponents from BO scaling, $\Delta\zeta_T(p)$ and $\Delta\zeta_u(p)$, are the same and $\log_2[xa^{1-p/3}+(1-x)b^{1-p/3}]$. As shown in Fig. 10, $\Delta\zeta_u(p)$ is somewhat larger than $\Delta\zeta_T(p)$ for large p. On the other hand, for small p, the former is somewhat smaller than the latter. As a result, even if we treat δ as a fitting parameter, both of the exponents $\zeta_T(p)$ and $\zeta_u(p)$ cannot be fitted accurately with Eqs. (24a) and (24b).

We cannot explain clearly why the second model is better than the first model. In the second model, in terms of the eddy viscosity, the temperature and velocity structure functions have the same dependence on the fragmentation parameter β. As a consequence, it prevents strong underestimation of the scaling exponents for velocity structure functions. Anyway, neither of the modified random-β models can sucessfully explain the intermittency in our shell model in the strict sense. In our shell model for convective turbulence, there exist inverse transfer of kinetic energy and large fluctuations of the flux functions, which sometimes cause a locally negative entropy flux. These coupled transfer processes are more complicated than the case of the 3D Navier-Stokes turbulence, so that the probability distribution $P(\beta)$ cannot be given by (21). This may be one of the reasons why the intermittency of the entropy and the energy dissipations observed in our shell model cannot be explained successfully by simple multifractal cascade models.

V. DISCUSSION AND CONCLUDING REMARKS

We have introduced an improved shell model for convective turbulence to study its statistical nature. Although our shell model has limitations compared with direct numerical simulation, it can reproduce the basic statistical quantities such as spectra and flux. Therefore, our model is helpful in understanding convective turbulence.

We confirmed that the energy and entropy spectra of our shell model are explained well by BO scaling. That is, convective turbulence is governed by the entropy cascade. Through the cascade process potential energy is converted into kinetic energy on average at every scales in the inertial range. A little of the kinetic energy is transferred to the dissipation range, but most of that is transferred to the larger scales. We infer that this inverse transfer of kinetic energy may play an important role in maintaining the robust circulation flow.

We have examined the intermittency appearing in the anomalous scaling of structure functions. In shell models the fractal is not substantial in the strict sense, because shell models give no information about physical space. Thus we should carefully compare the temporal "intermittency" obtained by the shell models with the multifractal cascade models.

The intermittency observed in the shell model for the 3D Navier-Stokes (NS) turbulence was well explained by the random-β-model [13]. We therefore introduced two modification of the multifractal cascade model for convective turbulence and compared them with the temporal intermittency in the shell model. One model assumes the local balance of the buoyancy term with the nonlinear term in the equation for velocity. It cannot fit well both the scaling exponents of the structure functions for temperature and velocity. The other model assumes the local balance of the buoyancy term with the eddy viscosity term. Both deviations in the scaling exponents from the BO values are roughly the same, so that the second model works much better than the first as the first approximation. However, the latter model also does not satisfactorily explain the details of the anomalous scaling for the structure functions. Although we do not clearly

understand the reasons for these failures so far, we point out the following aspects. In construction, our modified multifractal models do not explicitly deal with the direction of the energy flow. As discussed by Brandenburg, the inverse transfer of energy is essential for BO scaling. Then the direction of the energy flow might be considered in the modification of cascade models. Second, we cannot confirm that simple cascade models like ours really represent the anomalous scalings of structure functions even for temporal intermittency.

We also suggest that these failures might be due to stronger intermittency than that of NS turbulence. For shell models of NS turbulence, Jensen, Paladin, and Vulpiani [13] concluded that the largest Lyapunov exponents correspond to the temporal intermittency of the energy dissipation. Yamada and Ohkitani showed that Lyapunov functions for different values of dissipation agree with a function by rescaling with Kolmogorov entropy and Kaplan-York dimensions [16]. This suggests that the cascade process is governed by a simple scaling as a whole, including temporal intermittency. On the other hand, our shell model for convective turbulence does not possess such a similarity in Lyapunov functions as a whole [17]. However, if some of the largest Lyapunov exponents are removed and the same rescaling procedure is applied for the rest, the similarity is recovered. It should be noted that the number of largest Lyapunov exponents removed is dependent on κ. This suggests that for convective turbulence the intermittency is relatively stronger than that in NS homogeneous turbulence.

We also found another difference in power-law range between the inertial and dissipation ranges [18]. This extra range seems to possess a counterpart in the experimental results. As a matter of fact, for extremely large Rayleigh numbers the frequency spectrum of the entropy contains a complicated intermediate-dissipation range. It should be noted that this range is not scaled by the simple BO scaling [4]. We also tried to compare the spectra with a multifractal scaling, but they were not well fitted. The remarkable deviation from multifractal scaling is due to the existence of the precise length of extra range, that is, the wave number at which the power law predicted by BO scaling is replaced by extra range is scaled with κ in the same way as k_{θ_d}. Thus, only BO scaling works well even for the range above the dissipation range. However, this domination of Kolmogorov-type scaling over multifractal scaling is common to the shell model for the 3D NS turbulence we have studied. We have not explained clearly the relation between the intermediate-dissipation range and our extra range. In this sense, the intermittency examined in this paper does not seem compatible with experimental observations and multifractal scaling theory.

The extra range extends over two decades. The powers of the spectra in the extra range are close to the powers $-5/3$ and $-7/3$ for $S(k)$ and $E(k)$, respectively. The Boussinesq equation is unchanged under the following transformation in the inviscid limit: $\boldsymbol{x} \to \lambda \boldsymbol{x}$, $T \to \lambda^h T$, $t \to \lambda^{(1-h)/2} t$. Then, for h=1/5 we obtain the power laws predicted by BO scaling. On the other hand, the power laws in the extra range correspond to h=1/3. Although, as mentioned above, our spectra are not fitted well by multifractal scaling, scaling relations intrinsic to the Boussinesq equation are exhibited there. The multifractal scaling theory is based on the existence of these kinds of scaling relations. Therefore, we believe that our model contributes toward an understanding of the intermittency in turbulence.

Anyway, the intermittency in our model has not yet been compared with that in real convective turbulence. A study by wavelets on the intermittency of the two-dimensional model cited in Sec. II is under way. We will report the results in forthcoming papers.

ACKNOWLEDGMENTS

The authors would like to express their cordial thanks to I. Procaccia for valuable discussions and comments. This work was supported in part by a Grant-in-Aid (No. 06740341) from the Ministry of Education, Science and Culture of Japan.

[1] F. Heslot, B. Castaing, and A. Libchaber, Phys. Rev. A **36**, 5870 (1987).
[2] B. Castaing *et al.*, J. Fluid. Mech. **204**, 1 (1989).
[3] M. Sano, X.-Z. Wu, and A. Libchaber, Phys. Rev. A **40**, 6421 (1989).
[4] X.-Z. Wu, L. Kadanoff, A. Libchaber, and M. Sano, Phys. Rev. Lett. **64**, 2140 (1990).
[5] V. S. L'vov, Phys. Rev. Lett. **67**, 687 (1991).
[6] A. S. Monin and A. M. Yaglom, *Statistical Fluid Mechanics: Mechanics of Turbulence* (MIT Press, Cambridge, 1975), Vol. 2, p. 387.
[7] I. Procaccia and R. Zeitak, Phys. Rev. Lett. **62**, 2128 (1989).
[8] V. Yakhot, Phys. Rev. Lett. **69**, 769 (1992).
[9] A. Brandenburg, Phys. Rev. Lett. **69**, 605 (1992).
[10] S. Toh and E. Suzuki, Phys. Rev. Lett. **73**, 1501 (1994).
[11] S. Toh and E. Suzuki, *Unstable and Turbulent Motion of Fluid* (World Scientific, Singapore, 1993), p. 272.
[12] U. Frisch and M. Vergassola, Europhys. Lett. **14**, 439 (1991).
[13] M. H. Jensen, G. Paladin, and A. Vulpiani, Phys. Rev. A **43**, 798 (1991); **45**, 7214 (1992).
[14] R. Benzi, G. Paladin, G. Parisi, and A. Vulpiani, J. Phys. A **17**, 3521 (1984).
[15] R. H. Kraichnan, J. Atmos Sci. **33**, 1521 (1976).
[16] M. Yamada and K. Ohkitani, Phys. Rev. Lett. **60**, 983 (1988).
[17] S. Toh and E. Suzuki (unpublished).
[18] Of course, the intermittency studied here is derived from the structure functions estimated in the inertial range where the BO spectra, $S(k) \propto k^{-7/5}$, $E(k) \propto k^{-11/5}$, are clearly seen.